LDA MEASUREMENTS IN TURBULENT BOUNDARY LAYERS WITH ZERO PRESSURE GRADIENT

Gunnar Johansson
Department of Thermo and Fluid Dynamics
Chalmers University of Technology
SE – 412 96 Göteborg, Sweden
gujo@tfd.chalmers.se

Luciano Castillo
Department of Mechanical Engineering, Aeronautical Engineering & Mechanics
Rensselaer Polytechnic Institute
Troy, NY 12180 USA
castil2@rpi.edu

ABSTRACT

An experiment on zero pressure gradient turbulent boundary layers at low Reynolds number has been carried out. By combining LDA techniques and similarity analysis of the RANS equations the effects of upstream conditions on the downstream development of the mean flow and the turbulent quantities in the outer part of the boundary layer were investigated. It was found that for fixed upstream conditions, the mean velocity profiles collapsed to a single profile even though the local Reynolds number, R_θ, did not reach higher values than about 4000. The normal Reynolds stress profiles showed a marked dependence on local Reynolds number but also a tendency to collapse at the higher end of the local Reynolds number range considered. The Reynolds shear stress profiles depended strongly on local Reynolds number and showed only a weak tendency to collapse at higher Reynolds numbers. The effects of different upstream conditions were investigated by varying free stream speed and position and diameter of a trip wire. The mean velocity profiles and the streamwise normal Reynolds stress showed no dependence on the upstream conditions within the constraints of this experiment. The wall-normal Reynolds stress and the Reynolds shear stress, however, revealed a clear dependence on the position of the trip wire. Only the Reynolds shear stress showed a dependence on the trip wire diameter.

INTRODUCTION

Flat plate turbulent boundary layers have been studied for a very long time. Early investigations were made by, e.g., von Kármán (1930) and Millikan (1938), where the concept of similarity solutions to the turbulent boundary layer problem was introduced. Clauser (1954) extended this work to include boundary layers with pressure gradient. Basic experimental investigations were done by, e.g., Wieghart (1943) and Smith and Walker (1959).

Recent theoretical and experimental investigations include, e.g., George and Castillo (1997), Österlund (1999), and DeGraaff and Eaton (2000).

The complete solution for the mean velocity field for the idealized case of a perfectly flat, infinitely thin plate, perfectly aligned with a non-turbulent constant free stream can be expressed as

$$\frac{\langle U\rangle}{U_0} = f\left(\frac{y}{\delta}, \frac{xU_0}{\nu}\right) \qquad (1)$$

where $\langle U\rangle$ is the ensemble average of the streamwise velocity component U, U_0 is the constant free stream speed, $\delta = \delta(xU_0/\nu)$ is a boundary layer thickness, ν is the kinematic viscosity of the fluid and x and y are coordinates in the streamwise and wall-normal directions respectively. Similar expressions can be developed for the Reynolds stresses.

As the local Reynolds number, $R_x = xU_0/\nu$, goes to infinity, equation (1) loses its dependence on R_x, so that asymptotically

$$\frac{\langle U\rangle}{U_0} = f_\infty\left(\frac{y}{\delta}\right) \qquad (2)$$

This is, in fact, the Asymptotic Invariance Principle of George (1995).

The idealized case is, however, extremely difficult to achieve in practice, since neither infinitely thin plates, nor perfectly non-turbulent free streams exist. In order to control the transition to the turbulent state it has become common practice to use some tripping device, like a thin wire or a sandpaper strip. This, however, introduces new parameters into the problem and the general solution must now be written (for the case of a trip wire)

$$\frac{\langle U\rangle}{U_0} = h\left(\frac{y}{\delta}, \frac{xU_0}{\nu}, \frac{x_0U_0}{\nu}, \frac{x_0}{d_0}, *\right) \qquad (3)$$

where x_0 is the distance from the leading edge of the plate to the trip wire and d_0 is its diameter. A

possible dependence on other parameters, which cannot be controlled, like free stream turbulence, finite thickness of the plate and the shape of its nose, has been indicated by an unspecified set of parameters, denoted by *. We refer in the following to the complete set of parameters appearing in equation (3), but not in (1), as the "upstream conditions" of the flow field.

Even for different upstream conditions it is generally assumed that at sufficiently high local Reynolds numbers, R_x, the mean velocity field reduces to equation (2). For smaller local Reynolds numbers the dependence on the upstream conditions must be retained. It is the purpose of this paper to demonstrate how the mean velocity field and the Reynolds stresses vary with both the local Reynolds number and the upstream conditions for low to moderate local Reynolds numbers and to demonstrate that there is a tendency towards a universal form as the local Reynolds number increases. We will focus on the outer part of the boundary layer, i.e., on the functional form (3).

THE EXPERIMENT

A low Reynolds number experiment was carried out to test how the upstream conditions influence mean velocity profiles and Reynolds stresses. The turbulent boundary layer was 2-D, incompressible, steady state on the mean, and the flat plate was smooth. Details of the experiment are described below.

The Test Section

The measurements were carried out in the wind tunnel L2 in the department of Thermo and Fluid Dynamics at Chalmers University of Technology. The test section is 3 m long, 1.8 m wide and 1.25 m high. The corners are provided with fillets, slightly decreasing in size in the downstream direction to compensate for boundary layer growth on the wind tunnel walls. The wind tunnel is of conventional closed-loop design, equipped with turning vanes in all four corners with a number of honeycombs and screens. The contraction ratio is 5.6:1 and the free stream turbulence level is about 0.1%.

The experiment was made in two parts, both used the same flat plate, 2.5 m long, 1.25 m wide and 5 mm thick. A specially designed leading edge ensured that separation was avoided. In the first part the plate was mounted horizontally in the wind tunnel with the tip of its nose 200 mm downstream of the start position of the measuring section of the wind tunnel, and at a distance of 540 mm from the top wall of the wind tunnel. The boundary layer was tripped using a 2mm diameter wire, positioned at a distance of 150 mm from the leading edge and across the entire width of the plate. The free stream speed was varied from 5 m/s to 20 m/s. In the second part of the experiment the plate was mounted vertically at the centerline of the wind tunnel. Now also the position of the trip wire and its diameter were varied.

The LDA probes

Two LDA probes were used. One probe was used to emit four beams of blue and green light from an Argon-ion laser. Its focal length was 1200 mm and it was equipped with expanders to reduce the diameter of the measuring control volume to about 58 μm. A second probe was used to collect side-scattered light from the measuring control volume created by the 2D probe. With this side-scattering arrangement the measuring control volume was nearly spherical. For the Reynolds number range considered in this investigation the viscous length scale was estimated to vary from about 70 μm at the lowest to about 24 μm at the highest Reynolds numbers. Glass windows on the side and top walls of the wind tunnel facilitated optical access to the test section. In the second part of the experiment some profiles had to be obtained using backscatter, due to optical problems with these windows.

The scattered light was detected and processed by two Dantec BSA processors using the Burstware 3.22 program. With the present geometry of the beams the normal velocity component was measured in a direction slightly side-ways, making a small angle α to the normal, i.e., it was also somewhat sensitive to the transverse velocity component. The beam angles were measured to within 1°. The mean velocity in the normal direction could be corrected with very good accuracy based on the assumption that the transverse mean velocity is zero.

A potentially worse problem is created if the measurement of the normal velocity component is also sensitive to the velocity in the mainstream direction. This problem was avoided by performing test measurements very close to the wall ($y^+ \approx 2$), where the wall-normal velocity component is very close to zero. The probe was turned around its own axis until no mean velocity in the wall-normal direction could be detected.

Accurate determination of the distance between the measuring control volume and the wall is crucial, especially very close to the wall. The point of zero distance was determined by traversing the measuring control volume down to the wall, and seeking the vertical position where the scattering from the wall itself attained a maximum value. The correct wall-normal position could be determined to within 10 μm in this way, corresponding to 0.3 viscous wall units ($y^+ \approx 0.3$) at a free stream speed of 10 m/s. This process was repeated for each axial position.

RESULTS

Effects of the local Reynolds number

In figures 1-4 mean velocity profiles and Reynolds stress profiles are shown. The normal Reynolds stresses are shown as rms values. In these figures the upstream conditions are held constant,

$R_{x_0} = x_0 U_0/\nu \approx 100\ 000$, x_0/d_0=150. Only the local Reynolds number, $R_x = xU_0/\nu$, is varied.

The mean velocity profiles are hardly affected at all by the local Reynolds number, c.f. figure 1. Only for the lowest local Reynolds numbers a small deviation can be observed. We conclude that, for fixed upstream conditions, the mean velocity profiles approach the asymptotic profile already at very low local Reynolds numbers.

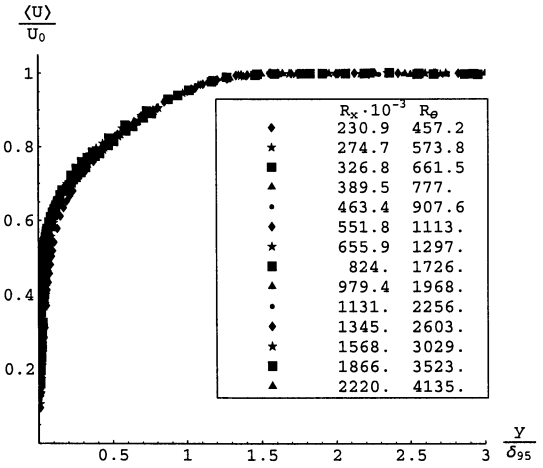

Figure 1: Mean velocity profiles obtained for $R_{x_0} \approx$ 100000, x_0/d_0= 150.

Profiles of the rms values of the stream wise velocity fluctuations, u_{rms}, are on the other hand strongly affected by the local Reynolds number, figure 2. The peak value close to the wall is the highest for the lowest local Reynolds number. For these profiles the position of the peak appeared at a dimensionless position farther away from the wall. One should also note that the difference between the different profiles extend almost all the way out to the free stream.

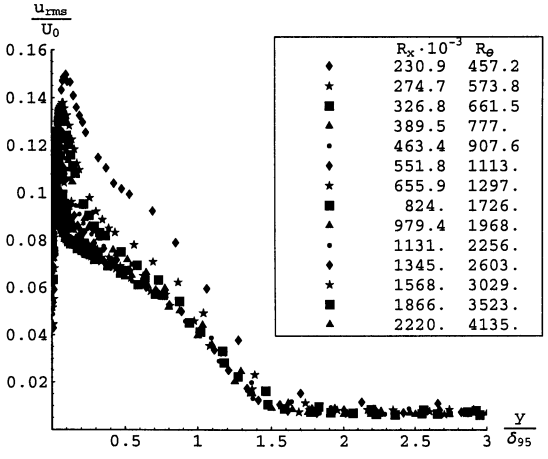

Figure 2: u_{rms} profiles obtained for R_{x_0} = 100000, x_0/d_0= 150.

The profiles for the rms values of the wall normal velocity fluctuations, v_{rms}, are shown in figure 3. They show a behavior similar to those of u_{rms}. There is a strong dependence on the local Reynolds number for the lowest ones. The peak values found here are lower than those found for the stream wise fluctuations and occurs farther away from the wall. As for u_{rms}, the position of the peak moves closer to the wall, in dimensionless coordinates, as the local Reynolds number increases.

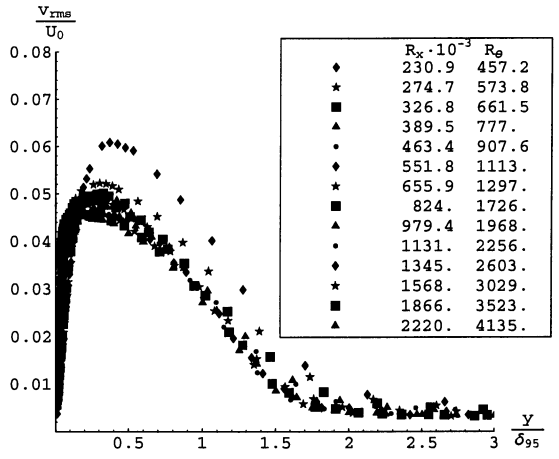

Figure 3: v_{rms} profiles obtained for $R_{x_0} \approx$ 100000, x_0/d_0= 150.

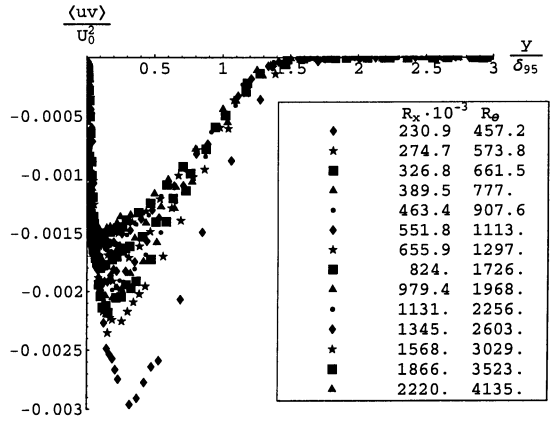

Figure 4: $\langle uv \rangle$ profiles obtained for $R_{x_0} \approx$ 100000, x_0/d_0= 150.

The Reynolds shear stress profiles, $\langle uv \rangle$, are shown in figure 4. The variation with the local Reynolds number is evident. For the smallest local Reynolds numbers a very strong negative peak is seen close to the wall. This peak appears at about the same position as the peak for v_{rms}. The behavior for increasing local Reynolds numbers is also similar, the magnitude of the peak value decreases and the peak position moves closer to the wall in dimensionless coordinates.

A careful inspection of figures 2-4 shows that the profiles for each of the Reynolds stresses tend to cluster together at higher local Reynolds numbers, thus, they seem to approach asymptotic profiles. For the fairly low local Reynolds number range reported here, neither the u_{rms}, v_{rms} nor the $\langle uv \rangle$ profiles can be claimed with certainty to have reached their asymptotic forms. Especially the $\langle uv \rangle$ profiles continue to vary throughout the range of local Reynolds numbers investigated here.

Effects of the trip wire position

Now we investigate the effects on the mean velocity and Reynolds stress profiles when the *global* Reynolds number based on the trip wire position, $R_{x_0} = x_0 U_0 / \nu$, is varied, while the *local* Reynolds number, $R_x = xU_0/\nu$, and the normalized wire diameter, x_0/d_0, are kept constant. Only a limited variation of global Reynolds numbers was covered in the present experiment.

Figure 5 shows the mean velocity profiles. As before, hardly any variation can be detected. It appears that the global Reynolds number R_{x_0} doesn't influence the mean velocity profiles at all. It should be stressed, however, that the empirical evidence presented here is far from sufficient to draw a final conclusion.

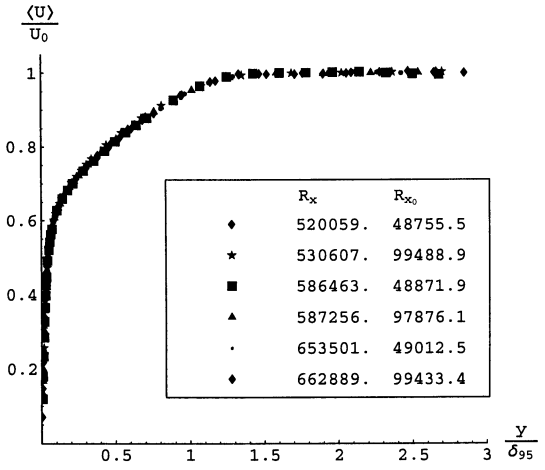

Figure 5: Mean velocity profiles for different global Reynolds numbers, R_{x_0}. x_0/d_0= 150 in all cases.

Figure 6 shows the profiles for the rms values of the stream wise velocity fluctuations for the same variation of local and global Reynolds numbers as in the previous figure. Although the global Reynolds number, R_{x_0}, varies by a factor of two no differences can be observed. We must conclude that a variation of the global Reynolds number, R_{x_0}, affects the u_{rms} profiles much less than the local Reynolds number variation does.

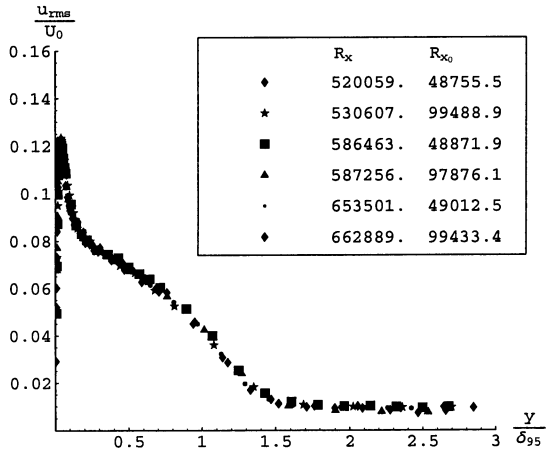

Figure 6: u_{rms} profiles for different global Reynolds numbers, R_{x_0}. x_0/d_0= 150 in all cases.

Figure 7 shows two pairs of profiles of the rms values of the wall-normal velocity fluctuations. In each pair the local Reynolds number is approximately the same but the global Reynolds numbers, R_{x_0}, are different. Contrary to the previous figures, here we can clearly see an effect of the global Reynolds number, R_{x_0}. Note that both profiles for the lower value of R_{x_0} lie above the profiles for the higher value.

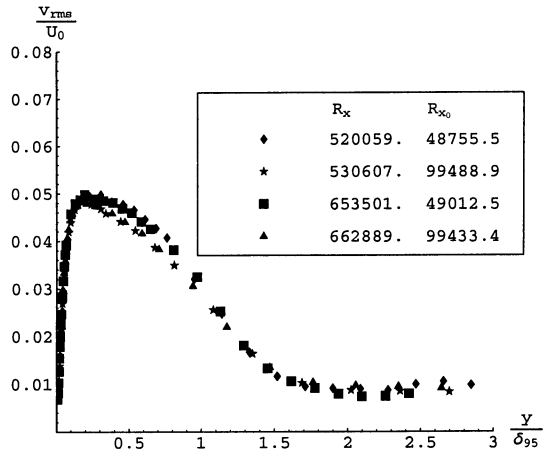

Figure 7: v_{rms} profiles for different global Reynolds numbers, R_{x_0}. x_0/d_0= 150 in all cases.

Figure 8 shows two pairs of profiles of the Reynolds shear stress. Each pair has approximately the same local Reynolds number but different global Reynolds numbers, R_{x_0}. As for the wall-normal velocity fluctuations we observe a dependence on the global Reynolds number. Note that the data points for the higher global Reynolds number fall above the data points for the lower ones regardless of local Reynolds number.

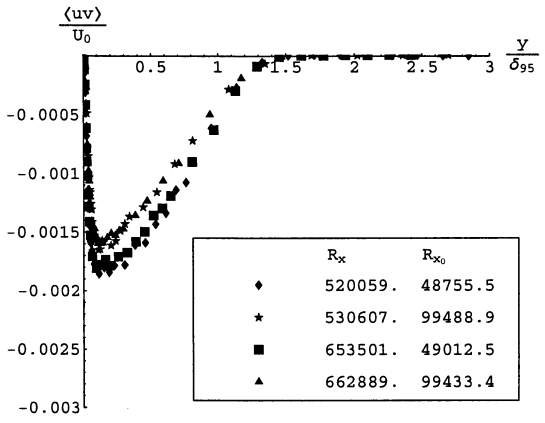

Figure 8: $\langle uv \rangle$ profiles for different global Reynolds numbers, R_{x_0}. x_0/d_0= 150 in all cases.

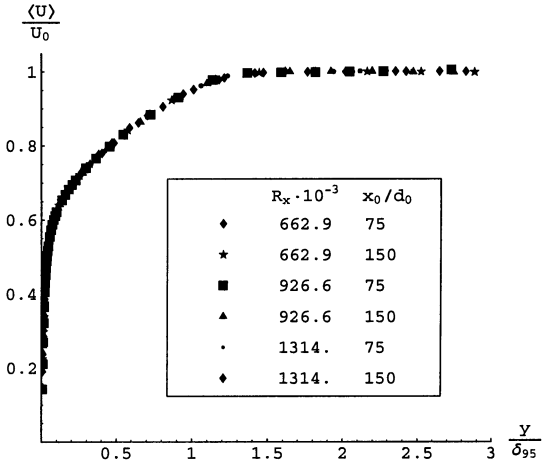

Figure 9. Mean velocity profiles for different x_0/d_0 ratios. R_{x_0} = 100000. Three pairs of data are shown.

In the investigation of the effects of trip wire position, the global Reynolds numbers, R_{x_0}, was varied by a factor of two, while the local Reynolds number variation was minor. The range of local Reynolds number is clearly too small to permit conclusions about possible asymptotic profile shapes. This holds true for any of the u_{rms}, v_{rms} and $\langle uv \rangle$ profiles.

Effects of the trip wire diameter

It is also of interest to find out to what extent the ratio x_0/d_0 affects the various boundary layer profiles. Figures 9-12 show profiles of mean velocity, u_{rms}, v_{rms} and $\langle uv \rangle$ for a constant global Reynolds number, R_{x_0} = 100000. Results are shown for three pairs of data. Within each pair of data the local Reynolds number is constant, but the ratio x_0/d_0 is different.

In figure 9 the mean velocity profiles for three sets of data with different x_0/d_0 ratio are presented. All six profiles fall on top of each other, indicating that the mean velocity profile is rather insensitive to variations in this ratio. As before a universal profile is obtained

Figure 10 shows profiles of the rms values of the streamwise velocity fluctuations for two values of the ratio x_0/d_0. It is virtually impossible to distinguish the different profiles from each other, indicating that these profiles are not sensitive to a change in this ratio. Close to the wall a slight broadening of the data can be seen. It is, however, not clear if this is mainly an effect of the x_0/d_0 ratio or the variation in local Reynolds number

Figure 11 shows how the profiles of the wall-normal velocity fluctuations are affected by the ratio x_0/d_0. No differences can be seen, which is somewhat surprising, since these profiles have shown a definitive sensitivity to both local and global Reynolds number variations. The deviations seen in

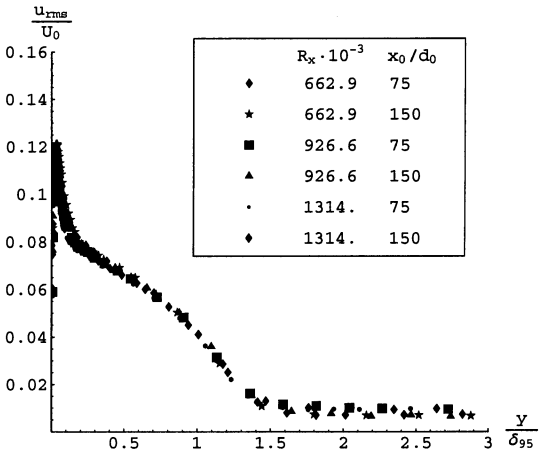

Figure 10. u_{rms} profiles for different x_0/d_0 ratios. R_{x_0} = 100000. Three pairs of data are shown.

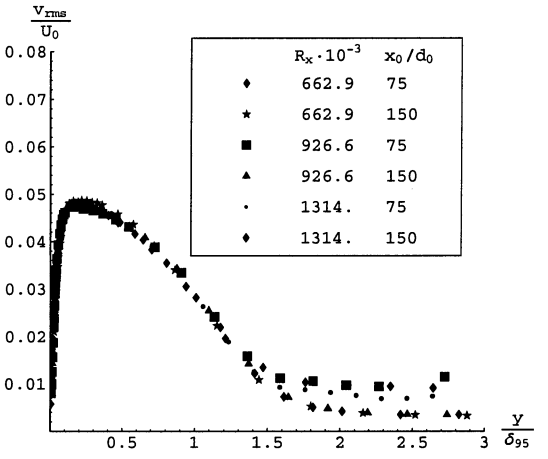

Figure 11. v_{rms} profiles for different x_0/d_0 ratios. R_{x_0} = 100000. Three pairs of data are shown.

the free stream are most likely due to measurement noise.

Figure 12, on the other hand, shows clearly that the Reynolds shear stress profiles are affected by a variation in the x_0/d_0 ratio. For each of the local Reynolds number values considered here, the Reynolds shear stress profiles for the higher value of x_0/d_0 fall below the profiles for the lower value. The difference between the profile pairs decreases for increasing local Reynolds numbers. The magnitude of the Reynolds shear stress is seen to decrease both with increasing local Reynolds number and with decreasing x_0/d_0 ratio. The Reynolds shear stress, thus, displays a dependence on the x_0/d_0 ratio, but this effect is intimately mixed with the effects of the local Reynolds number.

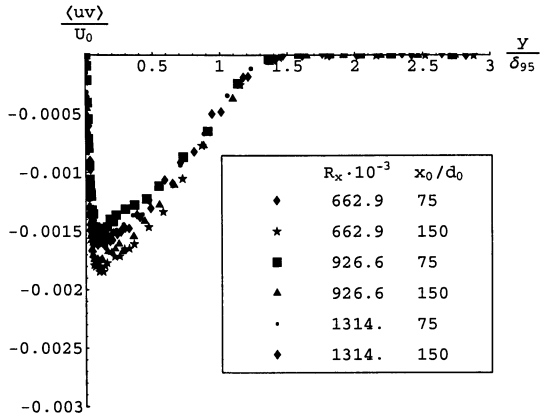

Figure 12:. $\langle uv \rangle$ profiles for different x_0/d_0 ratios. R_{x_0} = 100000. Three pairs of data are shown.

CONCLUSIONS

The main results from this low Reynolds number investigation are summarized below:

- The mean velocity profiles showed a weak dependence for low values of the local Reynolds number. However, already at a local Reynolds number of about 4000 an asymptotic profile was obtained. Within the limits of this experiment no dependence on either the trip wire position or its diameter could be detected.
- The stream wise velocity fluctuations, u_{rms}, showed a dependence on the local Reynolds number even for fixed upstream conditions. These profiles, though, showed a tendency to approach an asymptotic profile for the higher values of the local Reynolds number considered in this study. No dependence on either the trip wire position or its diameter could be found.
- The wall-normal velocity fluctuation, v_{rms}, also showed a dependence on the local Reynolds number, particularly for the lowest values of R_x. A tendency towards an asymptotic profile was also found, even for the low local Reynolds numbers studied here. Contrary to u_{rms}, however, v_{rms} showed a clear dependence on the position of the trip wire, but not on its diameter. This dependence did not show any tendency to decrease with increasing local Reynolds numbers, indicating a possible dependence on upstream conditions also of the asymptotic profile.
- For the Reynolds shear stress component, $\langle \rho uv \rangle$, the results were similar to v_{rms}. A strong dependence on the local Reynolds number was found, particularly for low values of R_x. For this variable only a very weak tendency towards a universal profile could be observed. This profile, if it exists, must be reached at significantly higher local Reynolds numbers than those investigated in this study. The Reynolds shear stress was found to be sensitive to variations in both the trip wire position and its diameter.

References

von Kármán, T., (1930), "Mechanische Ähnlichkeit und Turbulenz", *Nachr. Ges. Wiss.*, Göttingen, pp. 68.

Millikan, C.M., (1938), "A Critical Discussion of Turbulent Flows in Channels and Circular Tubes", *Proc. 5th Int. Congr. Appl. Mech.*, 386-392, Wiley, NY.

Clauser, F.H. (1954), "The Turbulent Boundary Layer", *Adv. Appl. Mech.*, IV, 1-51.

Wieghardt, K., (1943), "Über die Wandschubspannung in turbulenten Reibungsschichten bei veränderlichem Aussendruck", Kaiser Wilhelm Institut für Strömungsforschung, No.UM-6603, Göttingen, Germany.

Smith, D.W. and Walker, J.H., (1959), "Skin-friction measurements in incompressible flow", *NACA Rept.* R 26.

George, W.K. and Castillo, L., (1997), "Zero-Pressure Gradient Turbulent Boundary layer", *Applied Mechanics Reviews*, vol 50, no.12, part 1.

Österlund, J. M., (1999), "Experimental studies of zero-pressure-gradient turbulent boundary layer flow", Ph.D. Thesis, Royal Institute of Technology, Stockholm, Sweden.

DeGraaff, D. B. and Eaton, J. K., (2000), "Reynolds-number scaling of the flat-plate turbulent boundary layer", *J. Fluid Mech.* vol. 422, pp.319-346.

George, W.K.,(1995), "Some New Ideas for Similarity of Turbulent Shear Flows". *Turbulence, Heat and Mass Transfer*, ed. by K. Hanjalic and J.C.F. Pereira, (Begell House, NY).